Integration of pluripotency pathways regulates stem cell maintenance in the *Arabidopsis* shoot meristem

Ying Hua Su[a,b,1], Chao Zhou[a,1], Ying Ju Li[a,1], Yang Yu[a], Li Ping Tang[a], Wen Jie Zhang[a], Wang Jinsong Yao[a], Rongfeng Huang[c], Thomas Laux[b,d], and Xian Sheng Zhang[a,2]

[a]State Key Laboratory of Crop Biology, College of Life Sciences, Shandong Agricultural University, Tai'an, Shandong 271018, China; [b]Sino-German Joint Research Center on Agricultural Biology, Shandong Agricultural University, Tai'an, Shandong 271018, China; [c]Horticulture Biology and Metabolomics Center, Haixia Institute of Science and Technology, Fujian Agriculture and Forestry University, Fuzhou, Fujian 350002, China; and [d]Centre for Biological Signalling Studies, Faculty of Biology, University of Freiburg, 79104 Freiburg, Germany

Edited by Natasha V. Raikhel, Center for Plant Cell Biology, Riverside, CA, and approved August 5, 2020 (received for review July 21, 2020)

In the shoot meristem, both WUSCHEL (WUS) and SHOOT MERISTEMLESS (STM), two transcription factors with overlapping spatiotemporal expression patterns, are essential for maintaining stem cells in an undifferentiated state. Despite their importance, it remains unclear how these two pathways are integrated to coordinate stem cell development. Here, we show that the WUS and STM pathways in *Arabidopsis thaliana* converge through direct interaction between the WUS and STM proteins. STM binds to the promoter of *CLAVATA3* (*CLV3*) and enhances the binding of WUS to the same promoter through the WUS–STM interaction. Both the heterodimerization and simultaneous binding of WUS and STM at two sites on the *CLV3* promoter are required to regulate *CLV3* expression, which in turn maintains a constant number of stem cells. Furthermore, the expression of *STM* depends on WUS, and this WUS-activated *STM* expression enhances the WUS-mediated stem cell activity. Our data provide a framework for understanding how spatial expression patterns within the shoot meristem are translated into regulatory units of stem cell homeostasis.

shoot meristem | stem cell regulation | WUS–STM interaction

In multicellular plants and animals, stem cells are the ultimate source of new tissues and organs. Unlike higher animals, however, plants have the ability to form completely new organs, such as branches, leaves, flowers, and roots, throughout their life cycle. The establishment of plant architecture depends on both the shoot and root meristems residing at each end of the body to produce the aboveground and belowground organs, respectively. In the plant shoot meristems, divisions of the stem cells in the outermost layers provide the cells for all shoot structures. The daughter cells that stay in the central zone of the meristem renew the stem cell pool while the daughter cells that are displaced into the peripheral zone amplify further before becoming incorporated into the differentiating organ primordia.

Several decades ago, the isolation of meristem mutants revealed that stem cell homeostasis in the shoot meristem requires the input of two main regulatory pathways under the control of the homeodomain (HD) transcription factors WUSCHEL (WUS) and SHOOT MERISTEMLESS (STM), respectively. WUS was identified in *Arabidopsis* as a local specifier of stem cell identity (1, 2). The *WUS* gene is transcribed in a few cells in the shoot apical center, known as the organizing center (OC), located immediately below the three layers of stem cells (1). WUS protein migrates into the stem cells where it represses the differentiation genes and directly activates the transcription of the *CLAVATA3* (*CLV3*) gene (3–5). *CLV3* encodes a small peptide that acts as a feedback signal from the stem cells to the OC (6) where it delimits *WUS* expression and thus limits stem cell numbers (7, 8). The resulting WUS–CLV3 negative feedback loop between the OC and the stem cells underlies the dynamic regulation of stem cell homeostasis: Reduced *CLV3* activity results in stem cell overproliferation whereas its increase can cause the reduction or complete loss of the stem cells (7, 8). The TALE-homeodomain transcription factor STM is the *Arabidopsis* ortholog of the maize (*Zea mays*) KNOTTED1 protein (9, 10). *STM* is expressed throughout the shoot meristem, including the stem cells, the OC, and the transitioning amplifying daughter cells before they form organ primordia (9). It functions to repress cell differentiation and is therefore down-regulated in the incipient organ primordia.

The expression of *WUS* and *STM* in the stem cells acts to repress differentiation and activate *CLV3* expression (11, 12); however, the molecular mechanisms through which the WUS and STM regulatory inputs converge to regulate stem cell homeostasis are yet to be elucidated. Here, we show that both transcription factors directly interact with each other. STM directly activates *CLV3* transcription and interacts with WUS to enhance WUS binding to the *CLV3* promoter. *STM* expression is activated by WUS. The interaction between WUS and STM induces a sufficient CLV3 signal to negatively regulate *WUS* transcription, thus modulating the pool size of available stem cells.

Results

The Stem Cell Regulators WUS and STM Physically Interact with Each Other. Both WUS and STM are critical for the regulation of stem cells in the shoot meristem. Their expression patterns overlap in

Significance

Pluripotent stem cells are critical in both animal and plant development. Unlike higher animals, plants have unique postembryonic development, which continuously produce organs depending on shoot and root meristems. In the shoot meristem, division of the stem cells in the outermost layers provides the cells for all shoot structures. How those meristem cells are tightly controlled attracted intense studies. Genetic and molecular analyses in *Arabidopsis* have identified the key transcription factors WUSCHEL (WUS) and SHOOTMERISTEMLESS (STM) as the major regulators of pluripotency in the shoot meristem. Here, the results provide solid evidence showing how those two pluripotency factors WUS and STM coordinate to control shoot meristem cells strictly in plants.

Author contributions: Y.H.S. and X.S.Z. designed research; C.Z., Y.J.L., Y.Y., L.P.T., and R.H. performed research; W.J.Z. and W.J.Y. analyzed data; and Y.H.S., T.L., and X.S.Z. wrote the paper.

The authors declare no competing interest.

This article is a PNAS Direct Submission.

[1]Y.H.S., C.Z., and Y.J.L. contributed equally to this work.

[2]To whom correspondence may be addressed. Email: zhangxs@sdau.edu.cn.

This article contains supporting information online at https://www.pnas.org/lookup/suppl/doi:10.1073/pnas.2015248117/-/DCSupplemental.

First published August 24, 2020.

the OC and stem cells, and their ectopic coexpression can produce a synergistic effect in conferring a stem cell identity on differentiated tissues (12, 13). This indicates that WUS and STM may somehow interact in the regulation of stem cell development.

To illustrate how WUS and STM coordinately regulate stem cell development, we first tested the possibility of their direct protein–protein interaction. Using pull-down and yeast two-hybrid assays, we clearly showed that WUS proteins directly interact with STM proteins in vitro (Fig. 1 *A* and *B*). To further confirm their interaction, we tested the bimolecular fluorescence complementation (BiFC) following the transient expression of *STM-nYFP* and *WUS-cYFP* in tobacco (*Nicotiana benthamiana*) leaves, revealing their strong interaction compared with the negative controls (Fig. 1*C*). In these assays, SHORT ROOT (SHR) protein, which has been proven not to interact with WUS (14), was used as a negative control. In addition, we found that WUS was coimmunoprecipitated with STM in *Arabidopsis* protoplasts (Fig. 1*D*). Together, these results suggest that STM protein is a bona fide direct interactor of WUS in planta.

To determine the functions of the WUS and STM interaction, we overexpressed both *WUS* and *STM* (*SI Appendix*, Fig. S1) to examine their effects on *CLV3* expression. Consistent with their interaction, a 2-d overexpression of *35S::WUS-GR* and *35S::STM-GR* displayed a significant effect in up-regulating *pCLV3::GFP-ER* expression and increasing the shoot meristem size (*SI Appendix*, Fig. S2), in agreement with previous reports (11, 12). In order to genetically test WUS–STM function independently of the overexpression strategies, we combined hypomorphic genotypes since combinations of the *wus* and *stm* null mutations are difficult to interpret due to the strong growth defects of the single mutants. The microRNA-mediated reduction of *WUS* expression (*SI Appendix*, Fig. S1) in the weak stm_{bum1} allele strongly reduced its *CLV3* expression and increased the shoot meristem defects compared with the single mutants (Fig. 2). These findings confirm the genetic interaction of WUS and STM on *CLV3* expression and shoot meristem regulation.

In summary, we conclude that STM directly interacts with WUS and that both proteins can activate *CLV3* transcription. Because STM is expressed throughout the shoot apical meristem (SAM) dome and encompasses the WUS expression domain in the meristem center (*SI Appendix*, Fig. S3) (1, 9), the WUS–STM protein interaction could potentially occur in the OC and the apical stem cells.

WUS and STM Interaction Domains Are Essential for Their Functions. In order to test whether the physical interaction between WUS and STM is functionally relevant for *CLV3* transcription and stem cell regulation, we first identified the domains in both proteins that are essential for their interaction.

The WUS protein is composed of the HD, the conserved WUS-box, an EAR motif, and an acidic domain (15, 16) (*SI Appendix*, Fig. S4*A*). Deleting the acidic domain (D229–249, ΔWUS6) or the adjacent upstream interdomain region (D209–228, ΔWUS5) abolished the interaction with STM, as revealed using yeast two-hybrid assays (*SI Appendix*, Fig. S4*A*). In contrast, deleting the regions containing the HD, the WUS-box, the EAR motif, or any of the three other interdomain regions did not affect its binding to STM.

The STM protein consists of the HD, two conserved KNOX domains (MEINOX domains), and an ELK domain (17, 18) (*SI Appendix*, Fig. S4*B*). Deleting KNOX1 (D119–169, ΔSTM3), KNOX2 (D170–221, ΔSTM4), or the ELK (D262–283, ΔSTM6) domain abolished its interaction with the WUS protein, as determined using yeast two-hybrid assays (*SI Appendix*, Fig. S4*B*). In contrast, deleting the STM HD or any of the four interdomain regions had no effect on the WUS–STM interaction.

Previous studies have already shown that the KNOX1 and KNOX2 domains of STM are required for its stem cell regulation (17, 18) and that the deletion of the acidic domain in WUS

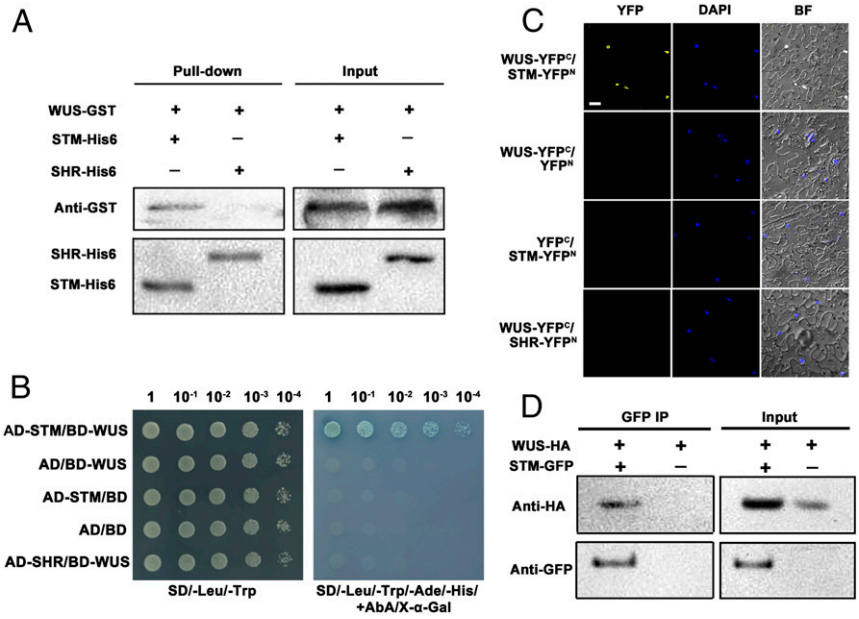

Fig. 1. Direct interaction between WUS and STM in vitro and in vivo. (*A*) Pull-down assay with STM-His_6 immobilized on an Ni Sepharose, showing that GST-WUS was retained by STM-His_6. (*B*) Yeast two-hybrid assay. The different protein combinations are listed on the left. The panels show 10-fold dilutions on media lacking leucine and tryptophan (–Leu, –Trp) or lacking leucine, tryptophan, adenine, and histidine (–Leu, –Trp, –Ade, –His), supplemented with AbA and X-α-Gal. (*C*) BiFC assay in tobacco epidermal cells. WUS interacts with STM (yellow nuclear signal). BF represents bright field. (Scale bar: 20 μm.) In *A*–*C*, SHR protein, which has been proven not to interact with WUS, was used as a negative control. (*D*) Coimmunoprecipitation assay. WUS was coimmunoprecipitated with STM in protoplasts. *35S::WUS-HA* and *35S::STM-GFP* were transiently coexpressed in *Arabidopsis* protoplasts. Single transformation of *35S::WUS-HA* was used as control. IP represents immunoprecipitation. Three independent repeats showed similar results.

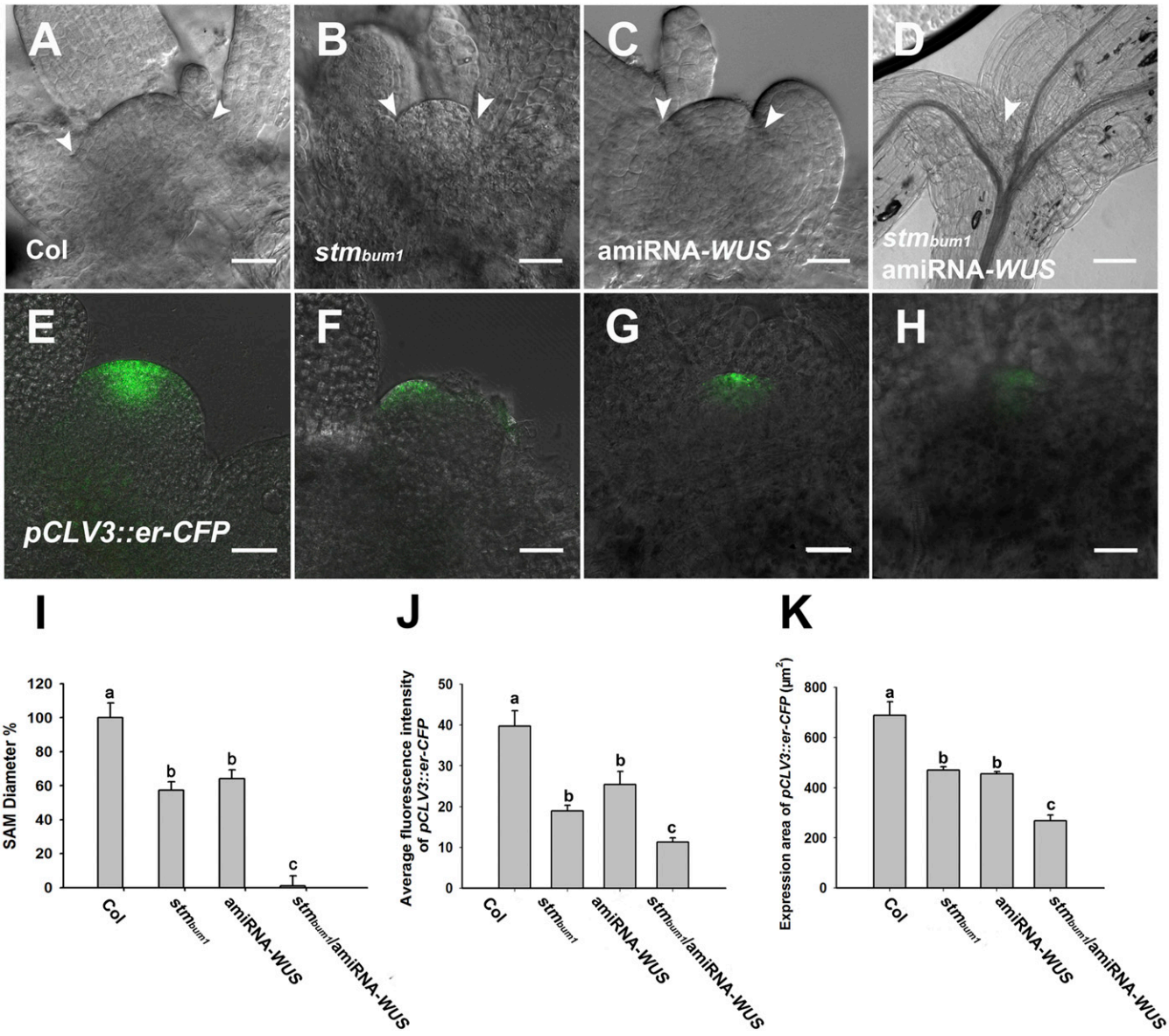

Fig. 2. The genetic interaction of WUS and STM in the SAM. (*A–D*) Differential interference contrast microscope images of the shoot apices of 10-d-old WT (*A*; Col, 84.6%, $n = 58$), *stmbum1* (*B*; 88.2%, $n = 59$), *35S::*amiRNA-*WUS* (*C*; amiRNA-*WUS*; 80.4%, $n = 56$), and *stmbum1*/*35S::*amiRNA-*WUS* (*D*; *stmbum1*/amiRNA-*WUS*; 96%, $n = 50$) plants. Arrowheads indicate the boundaries of SAM. (Scale bars: 50 μm.) (*E–H*) Images of *pCLV3::er-CFP* expression in the SAM of 10-d-old WT (*E*; Col, 84.5%, $n = 32$), *stmbum1* (*F*; 80.0%, $n = 40$), *35S::*amiRNA-*WUS* (*G*; 84.0%, $n = 38$), and *stmbum1*/35S::amiRNA-*WUS* (*H*; 95.1%, $n = 42$) plants. Green signals represent the *pCLV3::er-CFP*. Representative images of more than 10 independent transgenic lines. (Scale bars: 50 μm.) (*I*) SAM diameters, measured between the two arrowheads shown in *A–D*, presented as percentages of the WT SAM. (*J*) Fluorescence intensity of *pCLV3::er-CFP* expression in the SAM of 10-d-old WT (Col), *stmbum1*, *35S::*amiRNA-*WUS*, and *stmbum1*/*35S::*amiRNA-*WUS* plants. (*K*) Expression area of *pCLV3::er-CFP* expression in the SAM of 10-d-old WT (Col), *stmbum1*, *35S::*amiRNA-*WUS*, and *stmbum1*/*35S::*amiRNA-*WUS* plants. Bars in *I–K* indicate SE ($n \geq 30$ SAMs). Different letters in *I–K* indicate significant differences ($P < 0.01$), as determined using one-way ANOVA and Tukey's multiple comparison tests.

compromised the formation of stem cells in the shoot meristem during embryogenesis and inflorescence meristem activity (19). To reveal whether the STM ELK domain is also required for stem cell regulation, we expressed a mutant STM protein lacking the ELK domain (ΔSTM6) in the *stm* mutant. We found that *35S::ΔSTM6* expression was unable to restore the shoot meristem maintenance or *CLV3* expression, even in the weak *stm-2* mutant, whereas the full-length STM sequence complemented all mutant defects (*SI Appendix*, Fig. S5). This suggests that the ELK domain is required for the function of STM in stem cell regulation.

Together, these results show that the domains in either the WUS or STM proteins that are necessary for WUS–STM protein interaction are also important for *CLV3* transcription and/or stem cell maintenance. These results are consistent with the notion that the WUS–STM interaction plays an important role in regulating the shoot meristem.

Direct Binding of WUS and STM to the *CLV3* Promoter Is Required for *CLV3* Expression and Stem Cell Homeostasis. A previous study revealed that WUS directly binds to the *CLV3* promoter to regulate its expression (3). We therefore considered the possibility that the WUS–STM interaction directly promotes transcription from the *CLV3* promoter. This hypothesis was derived from the observation that the induction of *35S::STM-GR* activity

by a dexamethasone (DEX) application caused the up-regulation of *pCLV3::GFP-ER* after just 1 h, before the shoot meristem had increased in size, similar to the induction of the direct activator of *CLV3*, WUS-GR (*SI Appendix*, Fig. S6 *A–K*). Furthermore, this up-regulation of *pCLV3::GFP-ER* expression by either transcription factor alone or in combination was not altered by the presence of the protein biosynthesis inhibitor cycloheximide (CHX) (*SI Appendix*, Fig. S6*L*). To confirm that STM could act as a direct regulator of *CLV3* transcription, we performed chromatin immunoprecipitation (ChIP)–quantitative real-time PCR (qPCR) experiments using about 6,000 dissected shoot apices of plants expressing *pSTM::STM-VENUS*. We identified an enrichment of the S3 fragment of the *CLV3* promoter (−875 base pairs [bp] to −764 bp) (Fig. 3 *A* and *B*), which contains a predicted STM binding sequence TGACA (–797 bp to –793 bp) (20, 21). Using electrophoretic mobility shift assays (EMSAs), we found that STM binding to the S3 fragment was completely abolished when the TGACA motif was changed to TCTCA, and to a lesser extent if only one nucleotide was changed (Fig. 3 *C–E*). Together, these data strongly suggest that STM directly binds to the predicted TGACA motif of the *CLV3* promoter in *Arabidopsis* shoot apices.

To examine the role of STM binding to this motif for the regulation of *CLV3* transcription, we studied *GFP* reporter genes driven by different variants of the *CLV3* promoter. The *pCLV3m1::GFP* variant, in which the STM binding site is mutated to the aforementioned TCTCA, resulted in strongly reduced *CLV3* expression levels compared with the native *pCLV3::GFP* promoter (Fig. 4 *A*, *B*, *E*, and *F*) in the stem cells of the wild-type (WT) plants. This indicates that the STM binding site is required for normal *CLV3* promoter activity in shoot meristem stem cells. To analyze the requirement for STM binding in stem cell regulation, we expressed *CLV3* gene driven by the *CLV3m1* promoter variant in the *clv3-2* mutant. The *clv3-2* mutants typically exhibit a massive stem cell overproliferation in the shoot and floral meristems (6, 22) (Fig. 5 *A*, *B*, *G*, *H*, and *M*) and, as a consequence, produce 6.6 ± 0.4 carpels compared with the 2.0 ± 0.0 normally formed by WT plants (Fig. 5*N*). As expected, the expression of *CLV3* driven by its native promoter fully complemented the stem cell accumulation in the *clv3-2* mutant (Fig. 5 *C*, *I*, *M*, and *N*). In contrast, *pCLV3m1::CLV3* only partially suppressed the *clv3-2* defects (Fig. 5 *D*, *J*, *M*, and *N*). These findings strongly suggest that the STM binding site is required for normal stem cell homeostasis.

The identified STM binding site (−797 bp to −793 bp) in the *CLV3* promoter is about 285 bp from the reported WUS binding site containing a TAAT core motif (–1,082 bp to –1,079 bp) (3). In a ChIP analysis, protein extracts were isolated from 5,000 dissected shoot apices of 14-d-old seedlings expressing *WUS-GFP* driven by the endogenous *WUS* promoter, which has been shown to be fully functional (5). As a negative control, we used extracts from shoot apices expressing *35S::GFP*. We confirmed the enrichment of the (–1,156-bp to –989-bp) *CLV3* promoter fragment containing the WUS binding site (Fig. 6*A*). To investigate the developmental relevance of this motif, we mutated all four of the

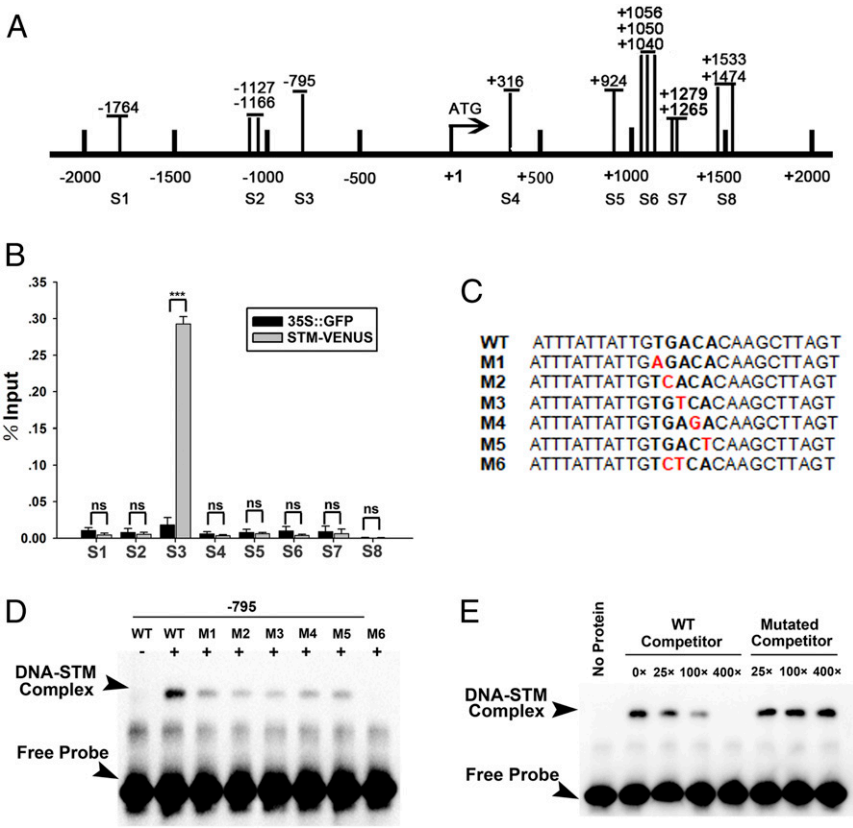

Fig. 3. STM protein directly binds to the *CLV3* promoter. (*A*) Sketch of the 2-kb region upstream and 2-kb downstream of the ATG codon (+1) of the *CLV3* gene. Several predicted STM binding sequences (TGACA) are indicated by horizontal bars. S1 to S8 indicate PCR fragments used for the ChIP-qPCR analysis. (*B*) ChIP-qPCR using an anti-GFP antibody in 14-d-old *35S::GFP* and *pSTM::STM-VENUS* seedlings. S1–S8 refer to the regions defined in *A*. Data represent means ± SD from three biological replicates. ***, $P < 0.001$ (Student's *t* test). ns, no significant difference. (*C*) Sequences of WT and mutated forms (M1–M6) of *CLV3* oligonucleotides from the –808-bp to –783-bp upstream region used for the EMSAs. The red letters represent mutated oligonucleotides. (*D*) Interaction between *STM* and *CLV3* oligonucleotides (WT and M1–M6 in *C*), determined using EMSA. (*E*) EMSA of the WT and M6 sequences shown in *C* revealing that the STM-DNA complex is reduced by an excess of WT *CLV3* but not *CLV3* M6 probes.

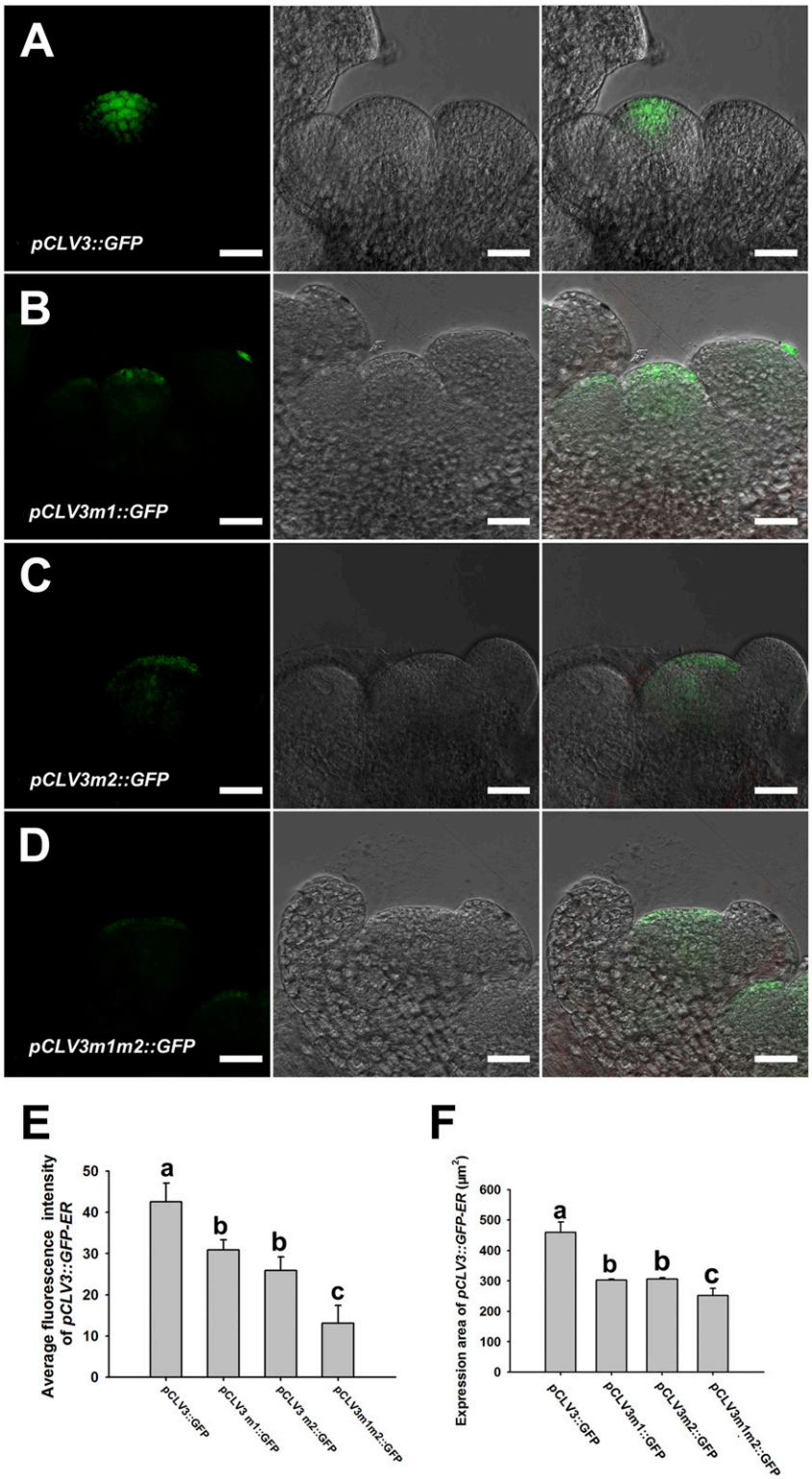

Fig. 4. STM and WUS binding sites are required for *CLV3* promoter activity. (*A*–*D*) Expression patterns of *pCLV3::GFP* (*A*; 90.1%, $n = 41$), *pCLV3m1::GFP* (*B*; 89.9%, $n = 39$), *pCLV3m2::GFP* (*C*; 91.2%, $n = 45$), and *pCLV3m1m2::GFP* (*D*; 90.8%, $n = 43$). (Scale bars: 50 μm.) Representative images of more than 10 independent transgenic lines. (*E*) Fluorescence intensity of *pCLV3::GFP*, *pCLV3m1::GFP*, *pCLV3m2::GFP*, and *pCLV3m1m2::GFP* in the SAM of 10-d-old seedlings. (*F*) Expression area of *pCLV3::GFP*, *pCLV3m1::GFP*, *pCLV3m2::GFP*, and *pCLV3m1m2::GFP* in the SAM of 10-d-old seedlings. Bars in *E* and *F* indicate SE ($n \geq 30$ SAMs). Different letters in *E* and *F* indicate significant differences ($P < 0.01$), as determined using one-way ANOVA and Tukey's multiple comparison tests.

TAAT nucleotides to GGGG (*pCLV3m2*) and found that this mutation severely reduced *CLV3* expression compared with the native *CLV3* promoter in stable transgenic plants (Fig. 4 *A*, *C*, *E*, and *F*). Furthermore, the expression of *CLV3* gene from *pCLV3m2* only weakly suppressed the *clv3-2* stem cell overproliferation phenotype compared with *CLV3* expression driven by its

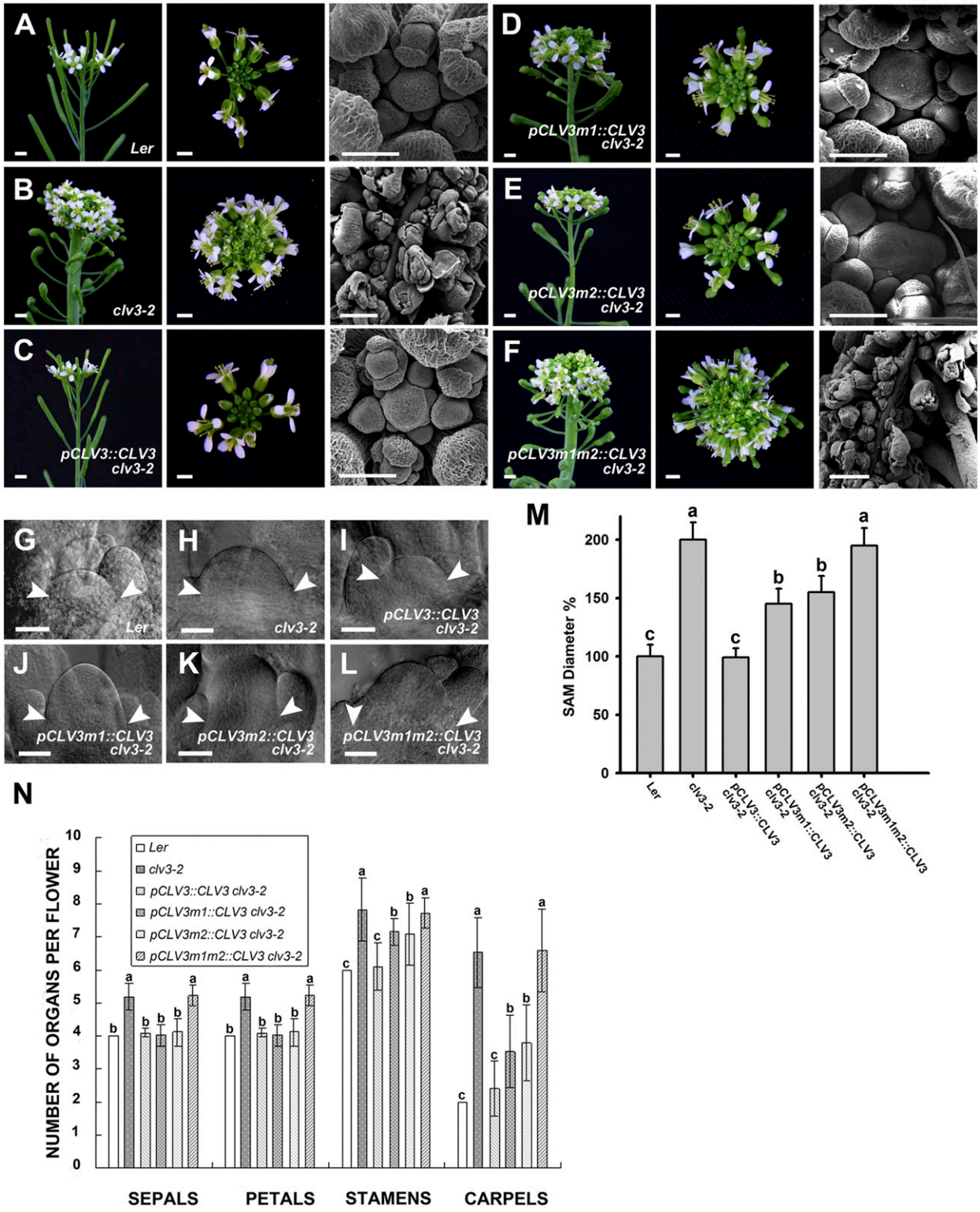

Fig. 5. STM and WUS binding sites are essential for *CLV3*-mediated stem cell control. (*A–F*) Photographs and scanning electron micrographs of the inflorescence meristems of the indicated genotypes: WT (Ler) (*A*; 85.0%, $n = 53$), *clv3-2* (*B*; 82.8%, $n = 58$), and *clv3-2* expressing *pCLV3::CLV3* (*C*; 82.2%, $n = 56$), *pCLV3m1::CLV3 clv3-2* (*D*; 81.2%, $n = 53$), *pCLV3m2::CLV3 clv3-2* (*E*; 85.6%, $n = 55$), or *pCLV3m1m2::CLV3 clv3-2* (*F*; 84.0%, $n = 56$). (Scale bars in photographs: 2 mm; scale bars in scanning electron micrographs: 500 μm.) (*G–L*) DIC images of the indicated shoot apices genotypes. Arrowheads indicate the boundaries of the SAM. (Scale bars: 50 μm.) (*M*) Diameters of the SAM measured between the two arrowheads shown in *G–L*, presented as percentages of the WT diameter. Bars indicate SEs ($n \geq 30$ seedlings). (*N*) Average numbers of floral organs in the indicated genotypes. Bars indicate SEs ($n \geq 40$ seedlings). In *M* and *N*, different letters indicate significant differences ($P < 0.01$), as determined using one-way ANOVA and Tukey's correction for multiple testing.

native promoter (Fig. 5 *E*, *K*, *M*, and *N*), confirming that the WUS binding site (–1,082 bp to –1,079 bp) is required for stem cell regulation.

Finally, the mutations at both binding sites (*pCLV3m1m2*) suppressed the reporter gene expression more than each single mutation (Fig. 4 *D*–*F*). The expression of *pCLV3m1m2::CLV3* could not complement the excessive stem cell accumulation phenotype in *clv3-2* (Fig. 5 *F* and *L*–*N*).

In summary, the binding sites of STM (−797 bp to −793 bp) and WUS (–1,082 bp to –1,079 bp) in the *CLV3* promoter are both required for *CLV3* expression and stem cell homeostasis.

WUS–STM Interaction Enhances WUS Binding to the *CLV3* Promoter. When we performed a ChIP analysis of the WUS-GFP protein from plants expressing both *pWUS::WUS-GFP* and *35S::STM-GR*, we noticed a strongly increased enrichment of the *CLV3* promoter fragment (–1,156 bp to –989 bp) containing the WUS binding site but not the STM binding site after a DEX induction (Fig. 6*A*). This raised the possibility that the presence of STM might enhance the binding of WUS to the *CLV3* promoter. By contrast, the coexpression of *pWUS::WUS-GFP* together with *35S::ΔSTM6-GR*, which cannot bind to the WUS protein, had no effect on WUS enrichment on the *CLV3* promoter (Fig. 6*B*), suggesting that this effect relies on a direct WUS–STM protein–protein interaction. Furthermore, we performed ChIP on dissected shoot apices of STM-VENUS expressed from the endogenous *pSTM* promoter and detected an enrichment of the *CLV3* promoter region containing the WUS binding site (–1,156 bp to –989 bp) but not the STM binding site (–797 bp to –793 bp) (Fig. 6*C*).

Using EMSA, we confirmed that the binding of WUS to a 26-bp fragment of the *CLV3* promoter (–1,090 bp to –1,065 bp), which contained the WUS binding site but not the STM binding site, was enhanced by the presence of STM (Fig. 6*D*). Importantly, STM did not bind this DNA fragment in the absence of WUS, as expected. Furthermore, the addition of STM resulted in a supershift of the WUS/DNA band (Fig. 6*D*). In contrast to the full-length STM, the ΔSTM6 deletion variant that is unable to bind WUS did not enhance WUS binding to the DNA fragment and did not cause a supershift (Fig. 6*E*).

Together, these results suggest that WUS and STM bind to the WUS target site as a complex and that the interaction with STM results in the increased binding of WUS to its motif in the *CLV3* promoter (–1,082 bp to –1,079 bp).

To address the consequences of this mechanism on the transcriptional regulation of the *CLV3* promoter, we then analyzed the effect of STM on the WUS-mediated expression from the *CLV3* promoter variant. The transient expression of *STM* fused with the *virD2* nuclear localization signal (NLS) in tobacco leaf cells was able to activate transcription of *LUC* from the *CLV3* promoter (*SI Appendix*, Fig. S7*A*) but had no activating effect on the expression of *pCLV3m1::LUC*, which contains a mutated STM binding site (*SI Appendix*, Fig. S7*B*), whereas the expression of *35S::NLS-STM* strongly enhanced the WUS-mediated *pCLV3m1::LUC* expression (*SI Appendix*, Fig. S7*B*). In summary, these results strongly suggest that the WUS–STM heteromeric complex binds to the (–1,082-bp to –1,079-bp) WUS binding site of the *CLV3* promoter and enhances transcriptional activity.

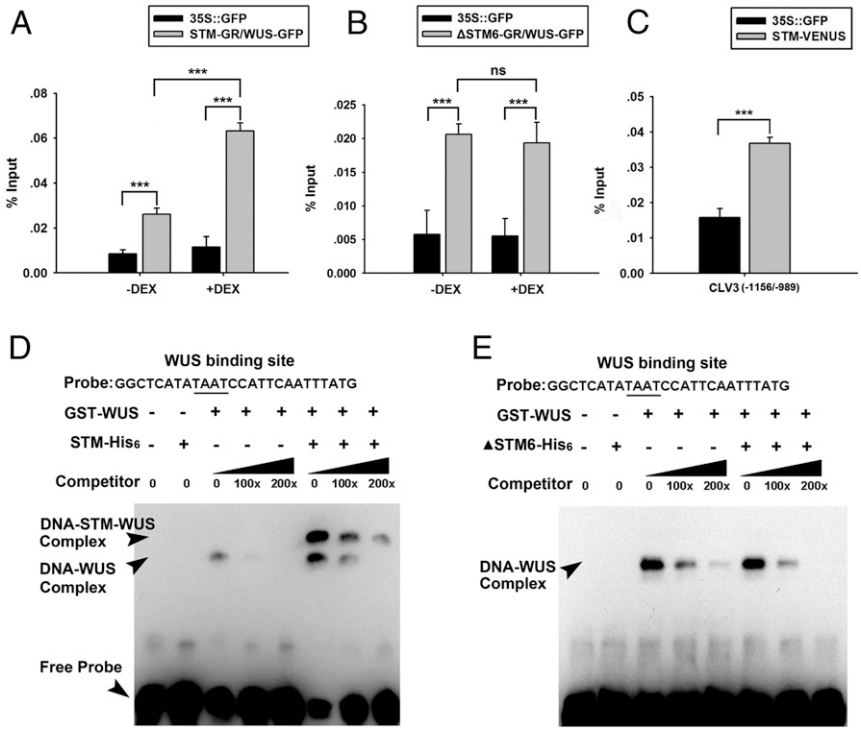

Fig. 6. STM enhances WUS binding to the *CLV3* promoter. (*A*) ChIP-qPCR of the –1,156-bp to –989-bp *CLV3* promoter region using an anti-GFP antibody to test samples from 14-d-old seedlings of *35S::GFP* or *35S::STM-GR/pWUS::WUS-GFP* (STM-GR/WUS-GFP). (*B*) ChIP-qPCR of the (–1,156-bp to –989-bp) *CLV3* promoter region using an anti-GFP antibody to test samples from 14-d-old seedlings expressing *35S::GFP* or *35S::ΔSTM6-GR/pWUS::WUS-GFP* (ΔSTM6-GR/WUS-GFP). (*C*) ChIP-qPCR of the (–1,156-bp to –989-bp) *CLV3* promoter region using an anti-GFP antibody to test samples from 14-d-old seedlings expressing *35S::GFP* or *pSTM::STM-VENUS* (STM-VENUS). (*D*) EMSA of WUS binding to a *CLV3* promoter region containing the WUS binding site (–1,065 bp to –1,090 bp) in the presence or absence of STM. Three biological replicates were conducted with similar results. (*E*) EMSA of WUS binding to a *CLV3* promoter region containing the WUS binding site (–1,065 bp to –1,090 bp) in the presence or absence of ΔSTM6 protein, lacking the ELK domain. Three biological replicates were conducted with similar results. Data in *A*, *B*, and *E* represent means ± SD from three biological replicates. ***$P < 0.001$ (Student's *t* test). ns, no significant difference.

WUS Activates *STM* Expression for Their Protein–Protein Interaction in the Shoot Meristem. As previously reported, STM is unable to induce *CLV3* transcription and stem cell maintenance in the absence of WUS activity (12). Further, STM activity is also known to be necessary to maintain a high level of *CLV3* transcription in the presence of WUS activity in the SAM (11). The functions of STM relating to *CLV3* transcription therefore depend on WUS. To address whether STM activation depends on WUS function, we analyzed the expression of *STM* in the SAM of STM-VENUS *wus-1* plants. *STM* expression was rarely detected in the SAM of the *wus-1* mutants (Fig. 7 *A* and *B*) because of the severe defects in the meristem cells. We further compared the signals of STM-VENUS in the SAM of the WT and artificial microRNA (amiRNA)-*WUS* plants. STM-VENUS fluorescence in the WT showed a concentrated distribution in the cells throughout the whole meristem (Fig. 7*A*). In the amiRNA-*WUS* plants, a strong reduction in STM-VENUS signals was detected, especially in the stem cell region and peripheral meristem regions, demonstrating that reduced WUS activity impairs the expression of *STM* in the stem cells (Fig. 7*C*). *WUS* overexpression in the WUS-GR plants promoted widespread *STM* expression, with strong signals detected in areas including the peripheral and inferior meristem regions that have early-differentiating cells (Fig. 7*D*). RNA in situ hybridization experiments also showed that the *STM* gene is transcribed in the central zone as well as in the peripheral and inferior SAM regions of DEX-induced *WUS*-overexpressing (WUS-GR) transgenic plants (Fig. 7 *E–H*). WUS therefore activates *STM* expression, which is in turn required for enhancing WUS-mediated stem cell activity through the WUS–STM interaction.

Discussion

Stem cell maintenance in plant meristems requires the coordination of multiple regulatory inputs to balance stem cell renewal and differentiation. In the shoot meristem, spatial patterns of gene activity underlie the dynamic regulation of stem cells and the transition of cell fates toward differentiation. How different inputs are integrated has been an enigma for decades. Here, we show that the pathways of two major transcriptional regulators, WUS and STM, converge by forming a heteromeric complex in the stem cells where the expression patterns of both genes overlap.

Our results show that STM can up-regulate *CLV3* transcription using two different mechanisms. STM binds to its canonical target sequence –797 bp to –793 bp upstream of the transcription start site, the deletion of which decreases *CLV3* promoter activity in the SAM. In addition, STM enhances the binding of WUS to the WUS binding site in the *CLV3* promoter (–1,082 bp to –1,079 bp) and becomes associated with this site in a strictly WUS-dependent manner, suggesting that both proteins bind DNA at this site as a heteromeric complex. It was reported previously that STM is unable to activate *CLV3* transcription in nonmeristematic cells lacking WUS activity (12), presumably because of its inability to heterodimerize with WUS. WUS activity is therefore required for the function of STM in *CLV3* transcription and stem cell maintenance. In contrast, *pCLV1::WUS* expression in *stm* mutants can induce the formation of an adventitious shoot meristem, but the meristems of these complemented plants grow much slower and reach smaller sizes than those expressing *pCLV1::WUS* with a WT background (7, 12), demonstrating that STM enhanced WUS-mediated stem cell activation. Our results reveal that STM acts synergistically with WUS to promote stem cell activity by strengthening the binding of WUS to the regulatory regions of the *CLV3* promoter. This effect is reminiscent of the interactions between animal TALE-HD and HOX proteins that increase the binding of HOX proteins to their target (23), suggesting a universal mechanism derived from the common ancestor of plants and animals.

Previous studies by Perales et al. identified several additional binding sites for WUS downstream of the *CLV3* coding region, revealing the highly complex nature of *CLV3* regulation (24). In their study, mutating all of these downstream elements reduced the *CLV3* promoter activity but did not abolish it, consistent with the presence of additional regulatory mechanisms identified here. In the same study, a single point mutation in the TAAT core motif of the WUS binding site at –1,082 bp to –1,079 bp did not appear to influence the *CLV3* expression pattern whereas deleting the region between –1,200 bp and –900 bp reduced the *CLV3* expression levels across the three stem cell layers. We therefore mutated all four nucleotides of this motif and found that the *CLV3* promoter activity was severely compromised in the driving of both *GFP* expression in the shoot meristem and *CLV3* expression in mutant complementation assays (Figs. 4 and 5). One possible explanation for the different results in these two studies might therefore be that a single nucleotide difference might be tolerated at this site.

The complexity of transcriptional *CLV3* regulation by WUS and STM raises the question of what may be the contribution of each factor. Mutating either the (–1,082-bp to –1,079-bp) WUS binding motif or the (–797-bp to –793-bp) STM binding motif resulted in similar reductions of *CLV3* promoter activity, as

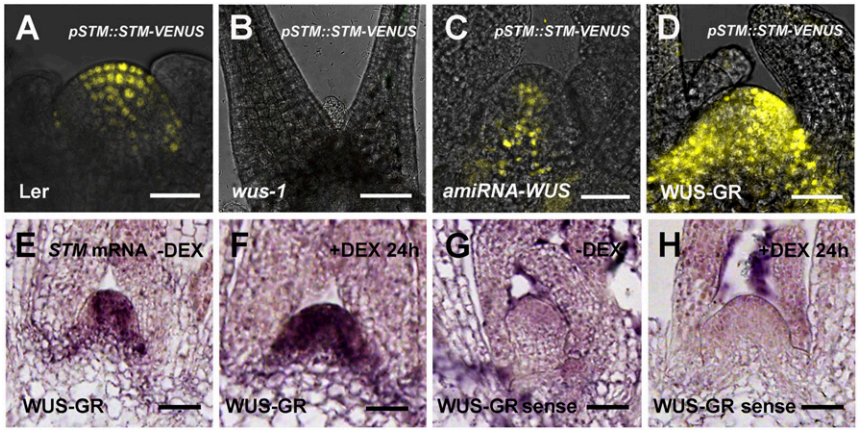

Fig. 7. WUS activates STM expression in the SAM. (*A–D*) *pSTM::STM-VENUS* expression in the SAM of 10-d-old WT plants (*A*; L*er;* 82.0%, $n = 45$), *wus-1* plants (*B*; 85.1%, $n = 34$), and amiRNA-*WUS* plants treated with estradiol for 10 d (*C*; 81.1%, $n = 37$), and *WUS-GR* plants after a day of DEX induction (*D*; 89.2%, $n = 46$). (Scale bars: 50 μm.) (*E–H*) Transcription of *STM* in 10-d-old *WUS-GR* plants with or without a day of DEX induction (DEX 24 h) in in situ hybridization assays. (Scale bars: 50 μm.)

demonstrated using reporter gene activity and *clv3-2* mutant complementation experiments, and we found stronger effects when both motifs were mutated (Figs. 4 and 5). This suggests roughly equal contributions of both transcription factors through the regulatory sites studied here, with a higher contribution of WUS being likely due to the additional regulatory site downstream of the *CLV3* coding region (24). Furthermore, it appears that the functions of both factors might vary between developmental stages. For example, whereas WUS is strictly required for the formation of the seedling shoot meristem and in flower development, other stages have a more relaxed requirement, as documented by the occasional postembryonic shoot growth (25), the bypass of the WUS requirement in certain mutant combinations (26), or the initiation of *CLV3* expression during embryogenesis in the absence of WUS activity (27). WUS is dispensable for embryonic stem cell formation since *CLV3* expression is initiated in the heart stage *wus-1* embryos; however, after the midembryo stage, WUS becomes indispensable for sustaining *CLV3* expression (27). At this stage, STM expression is induced, and its direct interaction with WUS likely contributes to the stem cell specificity function of WUS. Likewise, mutating the acidic domain of the WUS protein affects the formation of the seedling shoot meristem and the activity of the inflorescence meristem but enables the growth of postembryonic shoots (19). It is thus plausible that the contribution of WUS–STM varies during different developmental phases.

Curiously, STM is also expressed in the OC where the WUS concentration is the highest, but this does not lead to *CLV3* expression. Recent reports show that, in the OC cells, WUS interacts with the HAIRY MERISTEM (HAM) protein, which inhibits its ability to activate the transcription of *CLV3* by a currently unknown mechanism (14, 28). Together, our data suggest a model in which cell fates in the shoot meristem are regulated by combinatorial effects of transcription factors expressed in overlapping spatial patterns. In the stem cells, WUS and STM together maintain *CLV3* expression and stem cell identity whereas, in the OC, this function is blocked by HAM. In the meristem periphery, where WUS is absent, STM may prevent precocious differentiation and promote the separation of organ primordia. Finally, in the incipient organ primordia where neither *STM* nor *WUS* is expressed, differentiation can occur.

Materials and Methods

Plant Materials and Growth Conditions. All marker lines and mutants used in this study were in the Landsberg *erecta* (L*er*) or Columbia (Col) backgrounds. The following mutant alleles and transgenic lines were described previously: *wus-1* (L*er*) (2), *wus* (Col, GK870H12) (5), *stm-2* (L*er*) (29), *35S::WUS-GR* (L*er*) (30), *35S::STM-GR* (L*er*) (13), *pSTM::STM-VENUS* (L*er*) (31), *pCLV3::GFP-ER* (L*er*) (32), stm_{bum1} (Col) (33), and the *pWUS::WUS-GFP* lines (*wus* mutant rescue lines, Col) (5). *35S::WUS-GR*, *35S::STM-GR*, or *35S::WUS-GR*/*35S::STM-GR* were introduced into the *pCLV3::GFP-ER* reporter lines by crossing, and F_2 homozygous lines were used for imaging. To construct the *35S::STM stm-2* and *35S::ΔSTM6 stm-2* transgenic plants, the full-length complementary DNA (cDNA) of *STM* or *STM* lacking the ELK motif (*ΔSTM6*) was inserted into pCambia1300 between the KpnI and SalI sites. To generate the estrogen-inducible *35S::*amiRNA-*WUS* construct, the *WUS* gene fragments were amplified using PCR with the different combinations of primers shown in *SI Appendix*, Table S1. The amiRNA-*WUS* construct was cloned into an estradiol-inducible XVE binary vector, after which it was transformed into the Col (WT), stm_{bum1}, and *pSTM::STM-VENUS* genotypes. The *pCLV3::er-CFP* construct (27) was transformed into the Col, stm_{bum1}, amiRNA-*WUS*, and amiRNA-*WUS* stm_{bum1} plants.

All seeds were sterilized and plated on 0.8% (wt/vol) agar solid medium [half-strength Murashige and Skoog (MS) medium (34), supplemented with 1% sucrose and 0.05% 2-(*N*-morpholino)ethanesulfonic acid (MES), pH 5.7]. After a cold treatment to break dormancy, the seeds were grown under sterile conditions (light intensity of 40 μM photons·m^{-2}·s^{-1} at 20 to 22 °C with a 16-h light/8-h dark photoperiod). Two-week-old seedlings were transferred into soil and cultivated in a temperature-controlled chamber.

Coimmunoprecipitation Assays. The coding regions of WUS and STM were amplified and then inserted into the transient expression vectors *35S::HBT-HA-NOS* and *35S::HBT-GFP-NOS*, respectively. WUS-HA and STM-GFP were coexpressed in Col-0 protoplasts while single expression of WUS-HA was used as a negative control. Total proteins were extracted from the protoplasts with the extraction buffer (50 mM Tris·HCl [pH 7.5], 150 mM NaCl, 5 mM ethylenediaminetetraacetic acid [EDTA], 5% glycerol, 1% Triton X-100 with protease inhibitor, phosphatase inhibitor, and phenylmethylsulfonyl fluoride [PMSF]) and then incubated with GFP-Trap Agarose (catalog no. gta-20; ChromoTek) at 4 °C for 4 h, followed by two times of washing (50 mM Tris·HCl [pH 7.5], 150 mM NaCl, 5 mM EDTA, 5% glycerol, and 0.01% Triton X-100). Proteins were loaded into each well of a gel for sodium dodecyl sulfate polyacrylamide gel electrophoresis (SDS/PAGE). The immunoprecipitated proteins were analyzed using Western blotting with anti-hemagglutinin (HA) (catalog no. 12013819001; Roche) antibodies. STM-GFP were detected by an anti-GFP antibody (catalog no. HT801; TransGen) via Western blot.

Pull-Down Assays. The construct encoding the STM-His_6 or SHR-His_6 fusion protein was cloned into the pET-28a vector, and the construct encoding the GST-WUS fusion protein was cloned into the pGEX-4T vector. Recombinant GST-WUS and STM-His_6 proteins or GST-WUS and SHR-His_6 proteins were expressed in *Escherichia coli* BL21 (DE3) and purified as follows: One-tenth volume of precultured cells (5 mL) was added to 500 mL of fresh lysogeny broth medium and cultured at 37 °C until an optical density at 600 nm (OD_{600}) of 0.8 to 1 was attained. Protein production was induced by adding isopropyl-β-D-thiogalactopyranoside to a final concentration of 1 mM at 26 °C for 8 h. The bacteria were collected and centrifuged at 12,000 rpm, and the precipitate was added into 1× phosphate-buffered saline (PBS) buffer with PMSF. After sonication (10 s on, 15 s off, at 40% amplitude for 15 min), the expressed STM-His_6 or SHR-His_6 protein was purified using an Ni Sepharose 6 Fast Flow (catalog no. 17-5318-01; GE Healthcare), and the GST-WUS protein was purified with Glutathione Sepharose 4B (catalog no. 17-0756-01; GE Healthcare), according to the manufacturer's instructions. The purified proteins were stored at −80 °C until required. STM-His_6 or SHR-His_6 was immobilized on Ni Sepharose and incubated with GST-WUS or GST at 4 °C for 4 h. The agarose beads were washed three times with 1× PBS and processed for the SDS/PAGE and Western blot analyses using an anti-GST antibody (catalog no. M20007; Abmart). The pull-down experiments were repeated three times.

Yeast Two-Hybrid Assays. The coding region of the *WUS* gene and various *WUS* deletion derivatives were individually cloned into the pGBKT7 vector (catalog no. 630489; Clontech) between the EcoRI and BamHI sites, and the coding region of the *STM* gene, various *STM* deletion derivatives, and the *SHR* gene were cloned into the pGADT7 vector (catalog no. K1612-1; Clontech) at the same sites. Different combinations of bait and prey vectors were transformed into the yeast strain Y2H Gold and initially selected on synthetic complete medium lacking leucine and tryptophan (–Leu, –Trp). The protein interactions were then determined by measuring the growth of serial dilutions of transformed yeast cells on synthetic complete medium lacking leucine, tryptophan, adenine, and histidine (–Leu, –Trp, –Ade, –His) supplemented with AbA and X-α-Gal for 2 to 3 d. Each yeast two-hybrid assay was repeated at least three times.

BiFC Assays. The coding regions of *STM*/*SHR* and *WUS* were amplified using PCR with appropriate primers (*SI Appendix*, Table S1) and cloned into pSPYNE-35S and pSPYCE-35S, which contain DNA encoding the N- or C-terminal fusions of YFP (YFP^N or YFP^C), respectively. The two resulting constructs and the cotransformation vector 35S::P19 were transformed into the *Agrobacterium tumefaciens* GV3101 strain through electroporation. The *A. tumefaciens* strains were incubated, harvested, and resuspended in infiltration buffer (10 mM MES, 0.2 mM acetosyringone, and 10 mM $MgCl_2$) at a final concentration of OD_{600} = 1.0. Equal volumes of different combinations of *Agrobacterium* strains were mixed and injected into *N. benthamiana* leaves using a needleless syringe. The leaves were cultivated at 24 °C for 72 h prior to the detection of YFP fluorescence.

EMSAs. The EMSAs were performed as previously described (35). The expressed STM-His_6 protein and the GST-WUS protein were purified according to the methods described for the pull-down assays. WT and mutated oligonucleotides were commercially synthesized as single-stranded DNA. The WT oligonucleotide sequence corresponded to the −808-bp to −783-bp region of the *CLV3* promoter containing the STM binding site TGACA (20, 21). In the mutated oligonucleotide, TGACA (−797 bp to −793 bp) was replaced with TCTCA. To generate the double-stranded oligonucleotides,

equal amounts of complementary single-stranded oligonucleotides were mixed, boiled for 5 min, and then slowly cooled to 25 °C. A Light Shift Chemiluminescent EMSA kit (catalog no. 21048; Pierce) was used for the binding reaction.

ChIP Analyses. ChIP assays were performed as previously described (36), with some modifications. The shoot apices were dissected from 14-d-old *pSTM::STM-VENUS* or *pWUS::WUS-GFP* seedlings and were fixed in 1% formaldehyde in GB buffer (10% sucrose, 10 mM Tris HCl, and 1 mM EDTA) under a vacuum for 10 min at room temperature. After quenching the unreacted formaldehyde with glycine under vacuum for 5 min, the samples were ground in liquid nitrogen. Chromatin was isolated from the tissues, resuspended in SDS lysis buffer with protease inhibitors, and sonicated to achieve an average DNA size of 0.2 to 1.0 kilobases (kb). The lysate was precleared by an incubation with 50 μL of protein G agarose (catalog no. 16-201D; Millipore) for 1 h, followed by an incubation with anti-GFP antibodies (catalog no. SAB5300167; Sigma-Aldrich). The bound DNA fragments were then analyzed using qPCR. The DNA samples underwent 40 cycles of amplification, with the initial DNA concentrations being quantified from multiple samples in real time by analyzing the fluorescent signal intensities. qPCR was used to quantify the DNA in our samples using the primers shown in *SI Appendix*, Table S1.

Imaging Acquisitions. An Olympus JM dissecting microscope was used to photograph living seedlings, inflorescences, and flowers. For the scanning electron microscopy, the samples were treated, and micrographs were taken as described by Li et al. (37). Confocal microscopy images were taken using a Zeiss LSM 880 NLO confocal microscope with a 40× oil lens. The excitation and detection wavelengths for GFP, VENUS, and YFP were as previously described (32). To detect the CFP signals, a 458-nm laser was used for the excitation and a 470- to 535-nm long-pass filter was used for detection. Zeiss ZEN software was used to analyze the confocal images. For each marker line, at least 30 samples were imaged at each of the various developmental stages.

Chemicals and Induction. Estradiol (10 mM) stock solutions were dissolved in dimethyl sulfoxide (DMSO) and added to a half-strength MS solid medium (34) to a final concentration of 10 μM. The seedlings were grown on fresh medium containing estradiol every 3 d, for a total of 10 d for imaging. An equal volume of DMSO was added to the control medium.

DEX (catalog no. D4902; Sigma-Aldrich) was dissolved to a concentration of 5 mM in DMSO and stored at −20 °C. A final concentration of 5 μM in the half-strength MS solid medium was used for induction. CHX (catalog no. 239764; EMD Millipore Corp.) was dissolved to a concentration of 300 mM in DMSO and stored at −20 °C, and was used at a final concentration of 100 μM in half-strength MS solid medium for the inductions. To perform the inductions, the seedlings were grown on fresh medium for 10 d, after which they were transferred to a medium containing DEX or DEX and CHX for 1 h, followed by imaging. An equal volume of DMSO was added to the medium in the control experiments (Mock).

Transient Expression Assays in Tobacco. Transient expression assays were performed in *N. benthamiana* leaves, as previously described (38). The *CLV3* promoter (39) or its variant (*pCLV3m1*) was fused with the luciferase (LUC) reporter gene via the XhoI and BamHI sites of the pGreenII 0800-LUC vector (40) containing a *Renilla* luciferase (REN) driven by the *35S* promoter as an internal standard. The coding regions of the *WUS* or *STM* genes were fused to a pGreenII 62-SK vector downstream of the *35S* promoter between the restriction sites for BamHI and XhoI. The resulting plasmids were separately transformed into the *Agrobacterium* strain GV3101. Equal volumes of different combinations of *Agrobacterium* cells were mixed and coinjected into *N. benthamiana* leaves using a needleless syringe. After 4 to 5 d, the leaves were sprayed with 100 mM luciferin and placed in darkness for 5 min before their luminescence was detected.

A low-light, cooled, charge-coupled device imaging apparatus (IVIS Lumina II) was used for the image acquisition. Luminescence intensity was calculated using a previously described computational method (39). LUC and REN activities in the extracts were then measured using a Dual-Luciferase Reporter Assay system (E1910; Promega). The LUC activity was normalized to the REN activity.

Construction of *CLV3* Promoter Variants for the Complementation of *clv3-2*. The full-length *CLV3* genomic sequence including the *CLV3* coding region with 5′ upstream (1.8-kb promoter) and 3′ downstream (1.5-kb terminator) regulatory sequences was cloned into the pROKII vector between ClaI and SpeI (*pCLV3::CLV3*). To generate *CLV3* promoters containing mutations, site-directed mutagenesis was used to change the STM target motif TGACA (18, 20) at −795 bp to TCTCA (*pCLV3m1::CLV3*) and the WUS direct-binding site TAAT (3, 41) at −1,080 bp to GGGG (*pCLV3m2::CLV3*). The WUS and STM binding sites were also simultaneously mutated to generate *pCLV3m1m2::CLV3* constructs. The resulting constructs were separately transformed into *clv3-2* plants using the floral-dip method, as described by Clough and Bent (42).

Total RNA Isolation and Quantitative Reverse-Transcription PCR (qRT-PCR) Analysis. Total RNA was isolated from seedlings of 14-d-old seedlings using TRIzol reagent (catalog no. 15596-026; Invitrogen). The purified RNA was treated with DNase I (catalog no. EN0521; Thermo Fisher Scientific), after which the cDNAs were synthesized using Moloney Murine Leukemia Virus reverse transcriptase (catalog no. M1701; Promega). RNA quality was determined by examining the ratio of absorption at 260 nm and 280 nm using an ultraviolet spectrophotometer. The qRT-PCR reactions were performed for each cDNA dilution using SYBR Green Master mix with Chromo4, according to the manufacturer's protocol (Bio-Rad). The relative expression level of each gene was standardized to that of the housekeeping gene *TUBULIN2*. All of the primers used for the qRT-PCR are shown in *SI Appendix*, Table S1. The results were analyzed using the comparative C_T method, and the means and SDs were calculated.

Phenotypic Analysis and Measurement of the Shoot Meristems. To perform the microscopic analysis of the shoot meristem phenotypes, 10-d-old seedlings were fixed for 1 to 4 h in ethanol/acetic acid (6:1) at room temperature, as described previously (43). After washing in 100% ethanol followed by repeated washings in 70% ethanol, the seedlings were mounted in a mixture of chloral hydrate/glycerol/water (8:1:3) and cleared for ∼4 to 6 h at room temperature. The shoot meristems were then dissected, placed onto microscope slides, and mounted in a mixture of chloral hydrate/glycerol/water (8:1:3). Photographs of the samples were taken using an Olympus BX51 microscope. The size of each cleared shoot meristem was measured as a micrometer surface diameter for image analysis.

In Situ Hybridization. The in situ hybridization and detection of hybridized signals were performed as previously described by Zhao et al. (44), with some modifications. Antisense and sense RNA probes were labeled in vitro with cDNA fragments of *CLV3* or *STM* inserted into the *pEASY-Blunt3* vectors with digoxigenin–uridine 5′-triphosphate using SP6 and T7 RNA polymerases. The probes were subjected to an alkali treatment of 0.2 M $NaHCO_3$ and 0.2 mM Na_2CO_3, after which they were hydrolyzed to an average length of 150 nucleotides. The slides were hybridized with 200 ng/mL probes at 42 °C overnight in a hybridization solution containing 50% formamide. Hybridized probes coupled to an anti-digoxigenin antibody (conjugated with alkaline phosphatase) were used for the detection of the hybridized signals. Photographs were taken using an Olympus BX51 microscope.

Data Availability. All study data are included in the article and *SI Appendix*.

ACKNOWLEDGMENTS. This research was funded by the National Natural Science Foundation of China (31730008, 31670320, 31600157) and the Major Program of the Shandong Provincial Natural Science Foundation (2017C03).

1. K. F. X. Mayer *et al.*, Role of WUSCHEL in regulating stem cell fate in the *Arabidopsis* shoot meristem. *Cell* **95**, 805–815 (1998).
2. T. Laux, K. F. Mayer, J. Berger, G. Jürgens, The WUSCHEL gene is required for shoot and floral meristem integrity in Arabidopsis. *Development* **122**, 87–96 (1996).
3. R. K. Yadav *et al.*, WUSCHEL protein movement mediates stem cell homeostasis in the Arabidopsis shoot apex. *Genes Dev.* **25**, 2025–2030 (2011).
4. R. K. Yadav *et al.*, Plant stem cell maintenance involves direct transcriptional repression of differentiation program. *Mol. Syst. Biol.* **9**, 654 (2013).
5. G. Daum, A. Medzihradszky, T. Suzaki, J. U. Lohmann, A mechanistic framework for noncell autonomous stem cell induction in Arabidopsis. *Proc. Natl. Acad. Sci. U.S.A.* **111**, 14619–14624 (2014).
6. J. C. Fletcher, U. Brand, M. P. Running, R. Simon, E. M. Meyerowitz, Signaling of cell fate decisions by CLAVATA3 in Arabidopsis shoot meristems. *Science* **283**, 1911–1914 (1999).
7. H. Schoof *et al.*, The stem cell population of Arabidopsis shoot meristems in maintained by a regulatory loop between the CLAVATA and WUSCHEL genes. *Cell* **100**, 635–644 (2000).

8. U. Brand, J. C. Fletcher, M. Hobe, E. M. Meyerowitz, R. Simon, Dependence of stem cell fate in Arabidopsis on a feedback loop regulated by CLV3 activity. *Science* **289**, 617–619 (2000).
9. J. A. Long, E. I. Moan, J. I. Medford, M. K. Barton, A member of the KNOTTED class of homeodomain proteins encoded by the STM gene of Arabidopsis. *Nature* **379**, 66–69 (1996).
10. E. Vollbrecht, B. Veit, N. Sinha, S. Hake, The developmental gene Knotted-1 is a member of a maize homeobox gene family. *Nature* **350**, 241–243 (1991).
11. U. Brand, M. Grünewald, M. Hobe, R. Simon, Regulation of CLV3 expression by two homeobox genes in Arabidopsis. *Plant Physiol.* **129**, 565–575 (2002).
12. M. Lenhard, G. Jürgens, T. Laux, The WUSCHEL and SHOOTMERISTEMLESS genes fulfil complementary roles in Arabidopsis shoot meristem regulation. *Development* **129**, 3195–3206 (2002).
13. J. L. Gallois, C. Woodward, G. V. Reddy, R. Sablowski, Combined SHOOT MERISTEMLESS and WUSCHEL trigger ectopic organogenesis in Arabidopsis. *Development* **129**, 3207–3217 (2002).
14. Y. Zhou *et al*., Control of plant stem cell function by conserved interacting transcriptional regulators. *Nature* **517**, 377–380 (2015).
15. A. Haecker *et al*., Expression dynamics of WOX genes mark cell fate decisions during early embryonic patterning in *Arabidopsis thaliana*. *Development* **131**, 657–668 (2004).
16. E. van der Graaff, T. Laux, S. A. Rensing, The WUS homeobox-containing (WOX) protein family. *Genome Biol.* **10**, 248 (2009).
17. T. R. Bürglin, Analysis of TALE superclass homeobox genes (MEIS, PBC, KNOX, Iroquois, TGIF) reveals a novel domain conserved between plants and animals. *Nucleic Acids Res.* **25**, 4173–4180 (1997).
18. M. Cole, C. Nolte, W. Werr, Nuclear import of the transcription factor SHOOT MERISTEMLESS depends on heterodimerization with BLH proteins expressed in discrete sub-domains of the shoot apical meristem of Arabidopsis thaliana. *Nucleic Acids Res.* **34**, 1281–1292 (2006).
19. A. Dolzblasz *et al*., Stem cell regulation by Arabidopsis WOX genes. *Mol. Plant* **9**, 1028–1039 (2016).
20. L. Krusell, I. Rasmussen, K. Gausing, DNA binding sites recognised in vitro by a knotted class 1 homeodomain protein encoded by the hooded gene, k, in barley (Hordeum vulgare). *FEBS Lett.* **408**, 25–29 (1997).
21. S. V. Spinelli, A. P. Martin, I. L. Viola, D. H. Gonzalez, J. F. Palatnik, A mechanistic link between STM and CUC1 during Arabidopsis development. *Plant Physiol.* **156**, 1894–1904 (2011).
22. M. Lenhard, T. Laux, Stem cell homeostasis in the Arabidopsis shoot meristem is regulated by intercellular movement of CLAVATA3 and its sequestration by CLAVATA1. *Development* **130**, 3163–3173 (2003).
23. H. D. Ryoo, T. Marty, F. Casares, M. Affolter, R. S. Mann, Regulation of Hox target genes by a DNA bound Homothorax/Hox/Extradenticle complex. *Development* **126**, 5137–5148 (1999).
24. M. Perales *et al*., Threshold-dependent transcriptional discrimination underlies stem cell homeostasis. *Proc. Natl. Acad. Sci. U.S.A.* **113**, E6298–E6306 (2016).
25. P. Graf *et al*., MGOUN1 encodes an Arabidopsis type IB DNA topoisomerase required in stem cell regulation and to maintain developmentally regulated gene silencing. *Plant Cell* **22**, 716–728 (2010).
26. C. Lee, S. E. Clark, A WUSCHEL-independent stem cell specification pathway is repressed by PHB, PHV and CNA in Arabidopsis. *PLoS One* **10**, e0126006 (2015).
27. Z. Zhang, E. Tucker, M. Hermann, T. Laux, A molecular framework for the embryonic initiation of shoot meristem stem cells. *Dev. Cell* **40**, 264–277.e4 (2017).
28. Y. Zhou *et al*., HAIRY MERISTEM with WUSCHEL confines CLAVATA3 expression to the outer apical meristem layers. *Science* **361**, 502–506 (2018).
29. S. E. Clark, S. E. Jacobsen, J. Z. Levin, E. M. Meyerowitz, The CLAVATA and SHOOT MERISTEMLESS loci competitively regulate meristem activity in Arabidopsis. *Development* **122**, 1567–1575 (1996).
30. D. Lieber, J. Lora, S. Schrempp, M. Lenhard, T. Laux, Arabidopsis WIH1 and WIH2 genes act in the transition from somatic to reproductive cell fate. *Curr. Biol.* **21**, 1009–1017 (2011).
31. M. G. Heisler *et al*., Patterns of auxin transport and gene expression during primordium development revealed by live imaging of the Arabidopsis inflorescence meristem. *Curr. Biol.* **15**, 1899–1911 (2005).
32. S. P. Gordon *et al*., Pattern formation during de novo assembly of the Arabidopsis shoot meristem. *Development* **134**, 3539–3548 (2007).
33. B. Shi *et al*., Two-step regulation of a meristematic cell population acting in shoot branching in Arabidopsis. *PLoS Genet.* **12**, e1006168 (2016).
34. T. Murashige, F. Skoog, A revised medium for rapid growth and bio-assays with tobacco tissue cultures. *Physiol. Plant.* **15**, 473–497 (1962).
35. W. J. Meng *et al*., Type-B ARABIDOPSIS RESPONSE REGULATORs specify the shoot stem cell niche by dual regulation of *WUSCHEL*. *Plant Cell* **29**, 1357–1372 (2017).
36. Z. J. Cheng *et al*., Pattern of auxin and cytokinin responses for shoot meristem induction results from the regulation of cytokinin biosynthesis by AUXIN RESPONSE FACTOR3. *Plant Physiol.* **161**, 240–251 (2013).
37. Q. Z. Li, X. G. Li, S. N. Bai, W. L. Lu, X. S. Zhang, Isolation of HAG1 and its regulation by plant hormones during in vitro floral organogenesis in Hyacinthus orientalis L. *Planta* **215**, 533–540 (2002).
38. S. Song *et al*., Interaction between MYC2 and ETHYLENE INSENSITIVE3 modulates antagonism between jasmonate and ethylene signaling in Arabidopsis. *Plant Cell* **26**, 263–279 (2014).
39. M. Fiers *et al*., The CLAVATA3/ESR motif of CLAVATA3 is functionally independent from the nonconserved flanking sequences. *Plant Physiol.* **141**, 1284–1292 (2006).
40. R. P. Hellens *et al*., Transient expression vectors for functional genomics, quantification of promoter activity and RNA silencing in plants. *Plant Methods* **1**, 13 (2005).
41. E. Aichinger, N. Kornet, T. Friedrich, T. Laux, Plant stem cell niches. *Annu. Rev. Plant Biol.* **63**, 615–636 (2012).
42. S. J. Clough, A. F. Bent, Floral dip: A simplified method for *Agrobacterium*-mediated transformation of *Arabidopsis thaliana*. *Plant J.* **16**, 735–743 (1998).
43. T. Berleth, G. Jürgens, The role of the Monopteros gene in organising the basal body region of the Arabidopsis embryo. *Development* **118**, 575–587 (1993).
44. X. Y. Zhao, M. S. Liu, J. R. Li, C. M. Guan, X. S. Zhang, The wheat TaGI1, involved in photoperiodic flowering, encodes an Arabidopsis GI ortholog. *Plant Mol. Biol.* **58**, 53–64 (2005).